Quantifying and Modeling the Impact of Interconnection Failures on the Electrical Performance of Crystalline Silicon Photovoltaic Modules

Eleonora Annigoni[1], Alessandro Virtuani[1], Jacques Levrat[2], Antonin Faes[2], Matthieu Despeisse[2], Christophe Ballif[1,2]

[1] École Polytechnique Fédérale de Lausanne (EPFL), Institute of Microengineering (IMT), Photovoltaics and Thin Film Electronics Laboratory (PVLAB), 2000 Neuchâtel, Switzerland
[2] CSEM, PV-center, 2000 Neuchâtel, Switzerland

***Abstract* — We present an electrical model developed with LT-SPICE that simulates the performance of a string of cells with disconnections in the electrical circuit. In a previous contribution, we quantified experimentally how the module performance is affected when one or more ribbons are cut or disconnected between cells. The measurements were made on mini-modules (strings) of six cells, connected in series by three interconnection ribbons. Here, we use these experimental results to validate our model. Results show that our model is able to describe well the power reduction due to the interruption/removal of the cell interconnecting ribbons, and to reproduce the peculiar shape of the IV curves of a string affected by non-homogeneous distribution of the series resistance within some of the cells.**

***Index Terms* — PV module, interconnection failures, busbars, electrical model, reliability, crystalline silicon.**

I. Introduction

Series resistance increase is often observed in photovoltaic (PV) plants [1]. It can be the manifestation of different degradation mechanisms. For instance, the stress induced on the materials by accumulated thermomechanical fatigue (thermal cycles, wind or snow loads…) often affects the solder joints between the cell interconnect ribbon and the cell busbar. In some cases, fatigue can cause complete rupture of the ribbons and complete disconnection from the circuit. Furthermore, resistive solder bonds are, together with cell cracks, one of the causes of hot spots ([2] and [3]). In the extensive literature survey on PV module field reliability published in 2016 by Jordan et al. [4], hot spots and internal circuitry discoloration (caused by corrosion) are linked to high power losses and classified as the highest concerns for PV systems installed in the past 10 years.

Reliability of interconnect ribbons has gained more and more attention in the last few years. Many authors investigated the fatigue behavior of ribbons, by means e.g. of fatigue tests (see [5] among others). In [6], Bosco *et al.* propose a climate-dependent number of thermal cycles (according to IEC 61215) as a stress test for modules in order to obtain an equivalent amount of solder fatigue damage as estimated by Finite Elements Method simulations.

However, to our knowledge, there is no experimental study directly assessing the impact of broken interconnections on the electrical parameters degradation. This work is a continuation of the study presented in [7], where we quantified experimentally the impact of one or more disconnected ribbons on the electrical performance of a module. Here, we use these measurements to validate an electrical model, implemented in LT-SPICE that is able to simulate the performance of a module presenting broken interconnection ribbons.

II. Experimental Work

For the experimental work, as also described in [7], we laminated two equal strings, each with six solar cells (Al back surface field) connected in series with 1.70 x 0.17 mm copper ribbons coated with $Sn_{62}Pb_{36}Ag_2$. The cells are mono crystalline, p-based, with three busbars. They are encapsulated with a glass/backsheet construction with ethylene-vinyl acetate as encapsulant material. As backsheet we employ a 50 µm thick ethylene tetrafluoroethylene (ETFE) sheet. Such thin layer can be cut easily and therefore allows cutting the selected ribbon without the risk of damaging the adjacent cells. We then cut some selected ribbons in different positions within the string in order to assess the impact on the performance.

The strings were characterized initially and after each step by means of IV curve measurements with a LED-halogen based sun simulator replicating the AM1.5 spectrum. The series resistance (R_s) of the string is extracted by means of a linear fit in proximity of the open-circuit voltage. We use the value obtained, R_{oc}, which is generally higher than the true value of R_s of the mini-module, as an approximation for R_s.

III. The Electrical Model

Our model in LT-SPICE describes each 3-busbars cell as a network of 3 parallel sub-cells (see Fig. 1). Each sub-cell is modelled with a two-diode equation.

In order to account for the new electrical paths after the ribbon cuts, the series resistance of the cell is treated by separating the different contributions in two. The contributions given by the front and rear lateral grid resistances (R_{Gf} and R_{Gb}) are highlighted and represented separately in the circuit. Indeed, as they relate to the lateral transport, they are involved differently when one ribbon path is missing. The other contributions (e.g. the bulk series resistance), representing the

978-1-5386-8529-7/18/$31.00 ©2018 IEEE

internal cell resistance, are instead left in the series resistance that appears in the two-diode model.

The series resistance given by the ribbon is modelled via the R_{ribbon} term. Finally, two resistances ($R_{connector}$) are included to model the connectors used to measure the IV curve of the modules.

The diode parameters were extracted experimentally by measuring one of the cells of the strings. From a nonlinear fit of the IV curve we derived the following diode parameters: $J_{01} = 5.2 \cdot 10^{-10}$ A/cm^2, $J_{02} = 1.1 \cdot 10^{-5}$ A/cm^2, $R_{sh} = 40$ Ω·cm^2. The internal series resistance (free of grid contribution) was obtained from the fitting of the full module measurement yielding $R_s = 4$ mΩ·cm^2. As the cell is monofacial, $R_{G,f}$ corresponds to the resistance between two front busbar, and $R_{G,b}$ to the rear metal blanket resistance value between two rear side ribbons. A four-terminal measurement yielded $R_{G,f} = 25$ mΩ and $R_{G,b} = 1$ mΩ. As all ribbons are the same size, they are modelled by a single-value contribution $R_{ribbon} = 3$ mΩ. The only adjustable parameters is $R_{connector}$ induced by the crocodile connectors used during the IV measurement and that could not be measured. Experimental data were accurately fitted with $R_{connector} = 3$ mΩ.

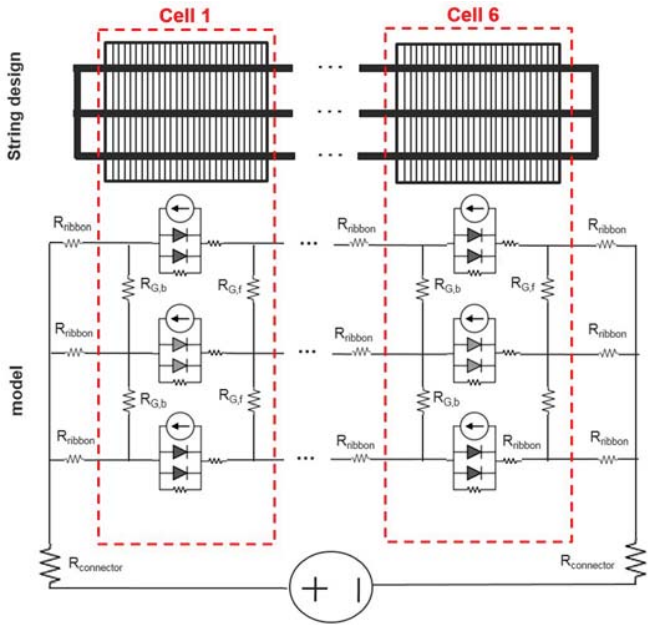

Fig. 1. Scheme of the electrical model developed in LT-SPICE to simulate the performance of a string with defective interconnecting ribbons. Cells from 2 to 5 are left out in this figure.

IV. Results

In the following sections, we present the results of the simulations and, by comparison with the experimental results presented in [7], obtain a validation of our model.

A. One Disconnected Ribbon Per Cell

Let us consider the case where the disconnections concern one ribbon per cell, and compare the impact on the module's electrical performance of broken external (Ext.) *vs* central (Cen.) ribbon. Fig. 2 displays the scheme of one of the strings used for this experimental work. Positions where the ribbons are cut are denoted by numbers (1,…,7).

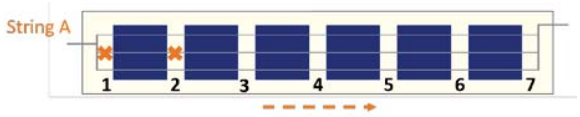

Fig. 2. Scheme of one of the six-cell strings used for the experimental work. In this case, the central (Cen.) ribbon is cut between consecutive cells (from point 1 sequentially to point 7). The same type of string is manufactured to analyze the case where one of the two externals (Ext.) ribbons is removed (String B, shown in Fig. 4).

Because of the difference between the front and the rear lateral grid resistances ($R_{G,f}$ and $R_{G,b}$), if the ribbon to the front side is cut first the performance degrades more than if the ribbon to the rear side is cut first. It is thus important to point out that the ribbons were disconnected starting from the front of the cell.

Fig. 3 shows the change in maximum power (P_{max}) of the full string after removing progressively one ribbon at a time from point 1 to 7, as measured (full circle symbols) and simulated (open squares symbols).

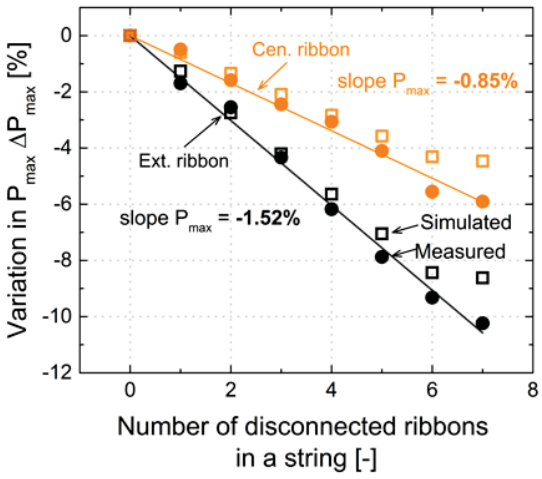

Fig. 3. Change in P_{max} with respect to the initial values (no disconnections) as function of the number of cumulative cuts. For instance, two disconnected ribbons means that the ribbon was disconnected in both positions 1 and 2 (see Fig. 2). The variation of the simulated values (open squares) follows closely the measured ones (full circles). Lines are linear fits of the measured values.

From the experimental work, we first observed that the P_{max} loss was entirely due to a loss in FF. The short-circuit current and the open-circuit voltage values remain unvaried after the disconnection of the ribbons. Moreover, the degradation depends on the position of the ribbon in the string. A larger impact on power loss was indeed measured when the external ribbon, rather than the central ribbon, was disconnected, with a power loss per cut of -1.51% and -0.85%, respectively.

Our simulations reproduce a variation of the P_{max} and of the FF (the last one not shown in the plot for the sake of clarity) in good agreement with the experimental results, with a relative error always less (in absolute value) than 1% for the P_{max} and 0.50% for the FF.

B. Two Disconnected Ribbons Per Cell

The mini-module used for the configuration where the external ribbon was cut (String B) was then employed to study the case where a second ribbon (the central one) is removed, see Fig. 4.

The measured variation in P_{max} is displayed in Fig. 5 (full circles), together with fitting lines. Here, the cuts in the central ribbon are plotted as consecutive to the previous cuts in the external ribbon (i.e. a cut in position n in the central ribbon corresponds to the x-coordinate $7+n$). The measurements showed that, after the external ribbon was completely removed (black dots), each cut in the central ribbon (blue dots) reduced the P_{max} by 3.76% (Fig. 5). With the external ribbon still connected, instead, the power loss was only 0.85%/cut (Fig. 3).

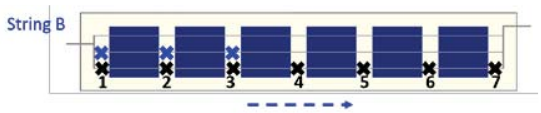

Fig. 4. Scheme of String B, used for the case of two disconnected ribbons per cell. First the external ribbon is sequentially cut, then a second ribbon per cell (the central one) is sequentially removed (8 to 14), one cell at a time.

In this case as well, the variation of the electrical parameters as function of the cumulated cuts obtained by our simulations (open squares) follows a trend that reproduces well the measurements. We show in Fig. 5 only the variation in P_{max}, the trend between experiment and simulations for the other relevant parameters such as fill-factor or R_s being analogous. In particular, the model simulates the change in the P_{max} slope that occurs as soon as the central ribbon starts to be disconnected too.

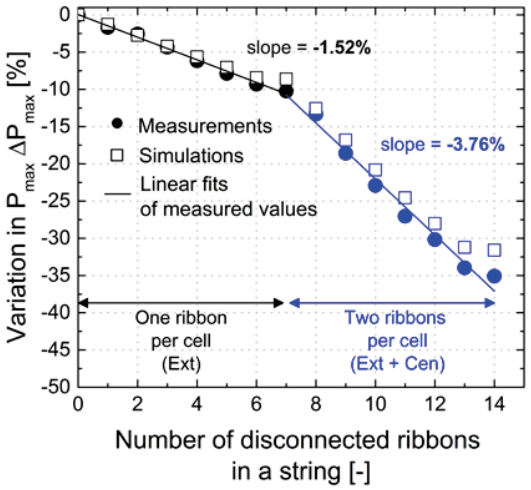

Fig. 5. Change in P_{max} with respect to the initial values (all ribbons connected) as function of the number of cumulative cuts, as measured and simulated.

The overlap between simulated and measured IV curves is also good (see Fig. 6). It is worth noticing that this simplified model is able not only to reproduce the variation in the curve slope close to the open-circuit point (correlated with R_s), but also the rounding at the maximum power point typical of the case where only part of the cell is affected by a high series resistance and part of the cell is not (inhomogeneous increase in R_s in the module). This effect was explained in [8]. A deviation is observed for a high number of cuts, i.e. in the presence of a strong deviation from the ideal behavior of the string. This issue is discussed in Section V.

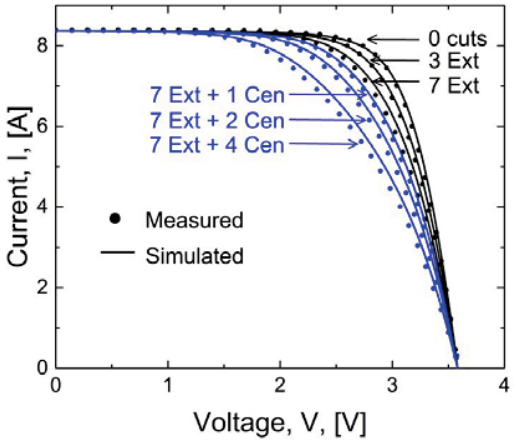

Fig. 6. IV curves for some of the configurations where two ribbons are removed per cell. Black curves: cuts in the external ribbon. Blue curves: the external ribbon is completely removed (points 1 to 7) and the central one is also cut.

Finally, we use the model to prove that the experimental results obtained on six-cell strings are scalable irrespective of the number of cells serially connected in a string. For example (these simulations are not shows here), if an external ribbon is disconnected from all cells in a string of 12 or 18 cells, the overall power loss will be approximately -10%, the same extent obtained in Fig. 3 for the string of six cells.

V. Discussion

Our model shows its limits when the induced series resistance becomes very high, in particular when two ribbons are disconnected per cell. This simple representation of the cell as 3 sub-cells in parallel and connected by the lateral grid resistance is not sufficient to fully reproduce the voltage distribution between terminals. However, the good agreement between our approach and the measurements, even with two missing ribbons, is encouraging and indicates that the main physical mechanisms have been seized.

This model, here validated experimentally, could be extended to simulate less extreme situations than broken ribbons, such as a series resistance increase due to resistive solder bonds. Moreover, it could be adapted to new metallization schemes such as cells with more busbars or advanced interconnection technologies (e.g. Meyer Burger's SmartWire Connection Technology SWCT®, [9]). It would then be a powerful tool to simulate modules with defective interconnections and predict the impact of such failures in new interconnection technologies.

VI. Conclusions

We start from a previous work where the effect of broken interconnection ribbons on the power performance of a PV module was quantified experimentally [7]. Some of the findings included the strong dependency of the power loss on the position of the ribbon within the string (central or external). As we cut one ribbon sequentially between adjacent cells, the string power decreased linearly at each cut. We quantified the slope of P_{max} as being -1.52%/cut if the external ribbon is removed, while only -0.85%/cut if the cuts are in the central ribbon.

Here, we present a model that simulates the electrical performance of a string with disconnected ribbons. Such model, developed in LT-SPICE, considers the cell as three sub-cells connected in parallel (three being the number of cell busbars), each sub-cell described by a two-diode model. The contributions to the R_s given by the lateral carriers transport on the grid (front and rear grid resistance) are treated separately from the R_s of the two-diode model, in order to account for the new electrical paths when one or more ribbons are missing.

A good agreement is found between the simulations and the measurements. The relative variation in the P_{max} (as well as FF and R_s, not shown here) after each cut is well reproduced. Moreover, the simulated IV curves follow closely the measured ones, also replicating the rounding at the maximum power point typical of inhomogeneous distribution of R_s in the cells. Larger deviations are observed in the simulated values when increasing the number of cuts (i.e. deviation from ideal behavior), and the limitations of this approach for studying such extreme cases are shortly discussed.

We then use the simulations to demonstrate that the experimental results are scalable irrespective of the number of serially-connected cells. The case where disconnections are distributed randomly within the module is also under investigation and will be subject of a future contribution.

We also discussed that the grid resistivity influences the power loss when one or two ribbons are disconnected. For example, when the ribbon to the rear side is cut first or when the ribbon to the front side is cut first. Therefore, having a strong grid can improve the reliability of the module against ribbon failure.

Acknowledgements

We gratefully acknowledge the financial support of EOS Holding and of the SCCER-Furies project (supported by CTI). We are grateful to Jonathan Champliaud for fruitful discussions and to Joël Sunier for support in the experimental work.

References

[1] IEA, "Review of Failures of Photovoltaic Modules - Report IEA-PVPS T13-01:2014," 2014.

[2] J. Muñoz , E. Lorenzo, F. Martinez-Moreno, L. Marroyo and M. Garcia, "An investigation into hot spots in two large grid-connected PV plants," *Progress in Photovoltaics: Research and applications,* vol. 16, no. 8, pp. 693-701, 2008.

[3] D. C. Jordan, T. J. Silverman, B. Sekulic and S. R. Kurtz, "PV degradation curves: non-linearities and failure modes," *Progress in Photovoltaics: Research and Applications,* vol. 25, no. 7, pp. 583-591, 2017.

[4] D. C. Jordan, T. Silverman, J., J. H. Wohlgemuth, S. R. Kurtz and K. T. VanSant, "Photovoltaic failure and degradation modes," *Progress in Photovoltaics: Research and Applications,* vol. 25, no. 4, pp. 318-326, 2017.

[5] R. Meier, S. Kraemer, S. Wiese, K.-J. Wolter and J. Bagdahn, "Reliability of copper-ribbons in PV modules under thermo-mechanical loading," in *35th IEEE Photovoltaic Specialists Conference (PVSC)*, pp. 1283-1288, 2010.

[6] N. Bosco, T. J. Silverman and S. Kurtz, "Climate specific thermomechanical fatigue of flat plate photovoltaic module solder joints," *Microelectronics Reliability,* no. 62, pp. 124-129, 2016.

[7] E. Annigoni, A. Virtuani, F. Sculati-Meillaud, A. Faes, M. Despeisse and C. Ballif, "Assessing the Impact of Broken and Defective Interconnection Ribbons on the Electrical Performance of Crystalline Silicon Photovoltaic Modules," in *33rd European Photovoltaic Solar Energy Conference and Exhibition*, pp. 1754-1757, Amsterdam, 2017.

[8] S. Bowden and A. Rohatgi, "Rapid and Accurate Determination of Series Resistance and Fill Factor Losses in Industrial Silicon Solar Cells," in *Georgia Institute of Technology*, 2001.

[9] T. Söderström, P. Papet and J. Ufheil, "Smart Wire Connection Technology," in *28th European Photovoltaic Solar Energy Conference*, pp. 495-499, 2013.